International Journal of GEOMATE, April, 2026 Vol.30, Issue 140, pp.140-147
ISSN: 2186-2982 (P), 2186-2990 (O), Japan, DOI: https://doi.org/10.21660/2026.140.g15395
Geotechnique, Construction Materials and Environment

EFFECTS OF INCREASING SOIL WATER CONTENT ON LIQUIDITY INDEX AND SLOPE FAILURE POTENTIAL THROUGH LABORATORY MODELLING

Nofrizal[1,2], * Fauzan[3], Abdul Hakam[3] ,Bambang Istijono[3], and Andriani[3]

[1] Civil Engineering Doctoral Student, Andalas University
[2] Padang Institute of Technology
[3] Department of Civil Engineering, Faculty of Engineering, Andalas University

*Corresponding Author, Received: 30 Aug. 2025, Revised: 26 Jan. 2026, Accepted: 28 Jan. 2026

ABSTRACT: This study investigates the influence of increasing soil moisture content on the Liquid Limit (LL), Liquidity Index (LI), and their subsequent effects on slope stability through controlled laboratory-scale physical modelling. Soil samples obtained from a landslide-prone area were initially characterized by index and consistency tests to determine their physical properties. The construction of slope models replicated the actual field condition at angles of 30°, 45°, and 60°, and was stimulated with a rainfall-induced failure scheme by progressive saturation. The main challenge found in the study was that changes in the Atterberg limits and Liquidity Index with rising moisture content in conventional slope stability assessment were frequently overlooked. Experimental results reveal that an increase in water content significantly elevates the Liquidity Index, with slope failures predominantly occurring when LI >1. Slopes with steeper angles, particularly those greater than 45°, indicates a significant reduction in shear strength and cohesion under the saturation stimulation, resulting in a high risk of instability. Furthermore, the results indicate that when water content exceeds the Liquid Limit, the soil structure rapidly degrades and transitions into a fluid-like state, causing it more vulnerable to flow-type failures. Also, the study provides empirical evidence encouraging the use of the Liquidity Index as a practical metric for assessing slope failure risk in fine-grained soils. By integrating Atterberg limit parameters with physical slope modeling, the study has managed to establish a simple, reliable, and cost-effective framework for evaluating rainfall-triggered landslide. In addition, the findings emphasize the critical importance of monitoring LI and LL values in steep, moisture-sensitive terrains as early warning indicators of slope instability.

Keywords: Index Properties Soil, Water Content, Liquid Limit, Slope Angle, Slope Failure

1. INTRODUCTION

Slope stability is the main concern in geotechnical engineering, specifically in the planning and design of infrastructure; highways, embankments, retaining structures, open-pit mines, and earth dams [1,2]. Slope failures can lead to severe consequences, including structural damage, causalities, environmental harm, and substantial economic losses [3–5]. Therefore, a reliable slope stability assessment is essential to mitigate these risks and ensure the durability and safety of the structures [6-8].

One of the primary factors contributing to slope instability is soil moisture variation, especially in regions with intense rainfall and poor drainage [9,10]. Changes in water content strongly influence the mechanical behavior of soils by modifying effective stress, shear strength, deformation characteristics, and pore water pressure conditions [11-15]. In cohesive soils, particularly clays, an increase in moisture content can significantly degrade mechanical strength and stiffness, making slopes more susceptible to failure.

For fine-grained soils, the consistency and plasticity properties are typically assessed through the Atterberg limits, which include the Liquid Limit (LL), Plastic Limit (PL), and Shrinkage Limit (SL) [16,17]. These parameters provide crucial information about how the soil behaves under different moisture levels. The Liquidity Index (LI), derived from the Atterberg limits, is a key indicator of soil consistency relative to its plastic range. When LI exceeds unity, the soil will be in the liquid-like state, indicated by extremely shear strength and an increased risk of slope failure [18].

Numerous studies have highlighted the role of water content and pore water pressure in triggering slope instability. Feng reported significant reductions in residual shear strength for cohesive soils when subjected to oversaturation conditions [19]. Troncone et al. developed topographic models that correlate the occurrence of shallow landslides with elevated groundwater levels [20]. Other studies emphasized the importance of matric suction and unsaturated soil mechanics in slope stability analyses [21-23]. Rahardjo et al. experimentally demonstrated that increasing saturation reduces suction effects, thereby accelerating slope failure in clayey soils [24]. Similarly, Sugimoto and Ishizuka and Nofrizal et al. showed that rainfall infiltration and groundwater fluctuations play a critical role in reducing slope safety factors and initiating landslides [25,26].

Despite advances in numerical modelling techniques and slope stability frameworks, the influence of moisture-induced changes in Atterberg limits and the Liquidity Index has been insufficiently explored in physical modeling studies. Conventional analyses typically assume invariant soil consistency parameters, thereby neglecting the progressive degradation of soil strength associated with increasing water content. To address this gap, the present study conducts controlled laboratory experiments to investigate the relationship between soil water content, Liquidity Index, and slope failure behavior.

The study focuses on soils from the Talamau Plateau in Pasaman Regency, West Sumatra (Fig.1), an area frequently affected by landslides due to its geological condition and substantial annual rainfall [27,28]. Annual precipitation in the region ranges between approximately 4,730 and 5,332 mm, combined with slope inclinations commonly exceeding 15°–30°, generating highly unfavorable stability conditions. These conditions make the Talamau region an ideal case study for examining rainfall-induced slope failure mechanisms.

Physical slope models were constructed at a 1:100 scale using field soil samples and tested under controlled rainfall conditions. The experiments were aimed to identify critical moisture thresholds, particularly when the Liquidity Index exceeds 1, and to evaluate the resulting deformation and failure mechanisms across different slope geometries. By establishing an empirical relationship of consistency parameters with slope behavior, this study provides a practical and field-applicable approach for assessing landslide susceptibility in fine-grained soils.

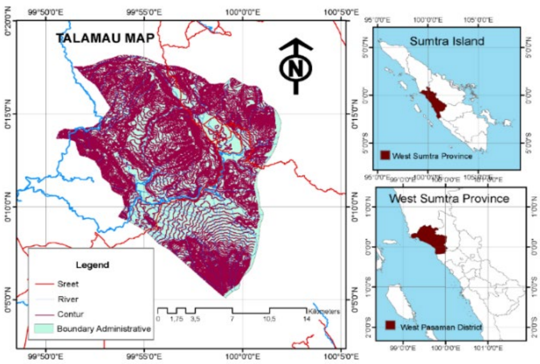

Fig.1 Geographical location of the Talamau Plateau landslide area of West Sumatra

2. RESEARCH SIGNIFICANCE

The primary significance of this study resides in the experimental verification of the Liquidity Index (LI) greater than 1 as a reliable and practical indicator of slope failure in fine-grained soils. By establishing a direct correlation between Atterberg limit parameters from the laboratory testing and the actual physical manifestation of slope failure, this research bridges the gap between conventional index testing and real-world slope instability phenomena. Unlike traditional slope stability assessments that assume constant soil consistency parameters, this study explicitly demonstrates how increasing soil water content alters the Liquidity Index and accelerates the transition from stable to unstable slope conditions.

3. MATERIAL AND METHOD

3.1 Study Area and Soil Sampling

This research was conducted on soils collected from landslide-susceptible zones in the Talamau Sub-district, Pasaman Regency, West Sumatra, Indonesia. The region is characterized by steep terrain, complex geological structures, and high annual rainfall, making it highly vulnerable to rainfall-induced slope failures. Field investigations identified critical unstable locations where silty clay soils dominate the near-surface layers**.**

Soil samples were collected using hand augers and core samplers at depths ranging between 0 and 1.5 m, representing the most weathered and failure-prone soil strata. The samples were transported to the Geotechnical Engineering Laboratory of Andalas University and the Soil Mechanics Laboratory of Padang Institute of Technology for comprehensive testing. Prior to laboratory analysis, the soils were air-dried, cleared of organic matter and coarse fragments, and sieved through a 2 mm mesh.

The physical and mechanical properties of the tested soils are shown in Table 1.

.

Table 1. Values of soil characteristics of test samples

Experiment	Parameters	Value	Units
Water content	w	60.594	%
Volume weight	γ	1,558	gram/cm^3
Specific gravity	Gs	2.627	
Sieve analysis	Gravel	0.000	%
	Sand	34.067	%
	Clay	65.933	%
Atterberg limit	SL	64.885	%
	PL	46.974	%
	PI	17.911	%
Direct shear	c	0.218	kg/cm2
	φ	22.835	°
Compaction	w opt	48.455	gram/cm3
	γ dry max	1.235	gram/cm3

Note: SL = Shrinkage Limit, PL = Non-elastic Limit, PI = Non-elastic Index, c = cohesion, φ = Inner shear angle, w opt = Optimum water content, γ dry max = dry soil specific gravity.

Index and physical property tests were conducted following ASTM standards, including natural water content (ASTM D2216), specific gravity (ASTM D854), unit weight, and Atterberg limits (ASTM D4318). The Liquid Limit (LL) and Plastic Limit (PL) values were subsequently used to calculate the Liquidity Index (LI), which serves as an indicator of soil consistency and its response to increasing moisture content.

3.2 Physical Slope Modelling

Semi-three-dimensional physical slope models were constructed at a scale of 1:100, with a uniform height of 34 cm and a base width of 30 cm. The models utilized the field soil compacted to 90% of the maximum dry density under dry conditions. Slope geometries of 30°, 45°, 60°, and 90° were selected to represent both natural and anthropogenic slopes commonly found in the study area.

Rainfall was simulated with a calibrated rainfall simulator equipped with ten oscillating nozzles, specifically designed to replicate local rainfall intensities. Throughout the experimental procedures, water infiltration, surface deformation, and slope failure mechanisms were continuously monitored. Soil moisture content was measured at regular intervals, and additional soil samples were collected during the tests to reassess Atterberg limits and calculate the corresponding Liquidity Index values. The slope model configuration and rainfall simulation setup are illustrated in Fig. 2(a) and Fig. 2(b), respectively.

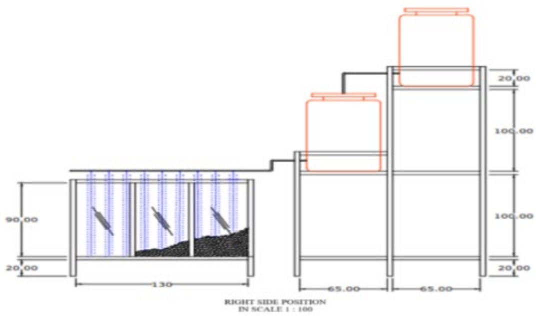

(a)

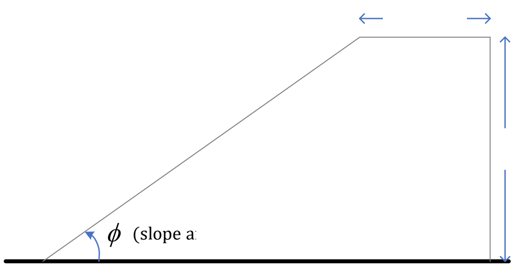

(b)

Fig. 2 Slope model. (a) Size of Landslide Model, (b) Slope Model Dimension

3.3 Experimental Framework

The experimental study was conducted to investigate the failure mechanisms of silty clay soils subjected to progressively increasing moisture conditions. The research methodology consisted of three primary stages.

Stage 1: Soil Characterization; this stage involved determining the physical and mechanical properties of the soil, including particle size distribution, specific gravity, bulk and dry unit weights, moisture content, and Atterberg limits (LL, PL, and PI). These parameters provided the fundamental basis for understanding soil consistency, plasticity, and moisture-induced behavior relevant to slope stability.

Stage 2: Slope Model Construction and Rainfall Simulation; in this stage, compacted soil samples were employed to construct slope models at specified angles. Controlled artificial rainfall was applied to simulate infiltration and saturation processes. Changes in soil moisture content were monitored over time, and soil consistency parameters were re-evaluated to assess the progression toward liquefaction and slope instability.

Stage 3: Stability Assessment and Failure Analysis; the final stage focused on evaluating the relationship between increasing water content, Liquidity Index evolution, and slope failure behavior. Changes in shear strength, cohesion, and internal friction were inferred from soil consistency transitions. The combined effects of moisture content, soil density, and slope geometry were analyzed to identify critical thresholds leading to deformation and collapse.

3.4 Water Content-Liquidity Index Relationship

In slope stability analysis, the interaction between water content, Liquid Limit, and soil mechanical properties is particularly critical for fine-grained soils. As water content increases and approaches or exceeds the Liquid Limit, soil cohesion and internal friction angle decrease significantly due to reduction of particle bonding and loss of matric suction. This behavior is quantitatively captured by the Liquidity Index (LI), defined as:

$$LI = \frac{w-PL}{LL-PL} \quad (1)$$

where w is the natural water content, PL is the plastic limit, and LL is the liquid limit. Values of LI less than zero indicate stiff or semi-solid soil, values between 0 and 1 correspond to plastic behavior, and values exceeding 1 represent a liquid-like state. Variations in LI during rainfall simulation directly reflect the degradation of soil shear strength and play a critical role in slope failure initiation.

The variations of LI significantly affect soil unit weight, cohesion, and internal friction, and are therefore critical for evaluating slope stability under rainfall infiltration conditions. The temporal evolution of the Liquidity Index (LI) during rainfall simulations is illustrated in Fig. 3, highlighting the progressive relationship between increasing moisture content and soil liquidity. The corresponding LI values for different soil conditions and slope configurations can be seen in Table 2, providing a quantitative basis for assessing slope failure susceptibility in landslide-prone areas.

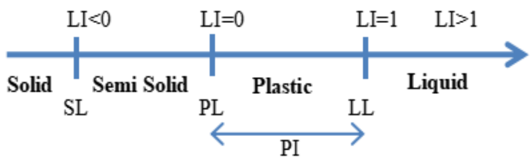

Fig. 3 Soil Liquidity Index Graph

Table 2. Quantitative basis for assessing slope failure susceptibility [29]

Items	Description
LI< 1	Semi-solid soil, high strength
0< LI < 1	Plastic state soil, medium strength, soil is a kind of plastic material
LI > 1	Soil begins to lose consistency, approaching liquid state, soil is liquefiable.
LI > 1.5	Very soft/liquid soil means that the water content of the soil is higher than its liquidity limit, so the soil behaves like a liquid and loses its cohesion.

4. RESULTS AND DISCUSSION

4.1 Soil Properties and Grain Size Distribution

The results of the sieve analysis on the soil samples used in the slope modelling experiments are presented in Table 3. Particle size distribution plays a critical role in evaluating soil behavior, particularly concerning permeability, plasticity, and susceptibility to slope failure. The soil samples were in grain sizes ranging from 4.75 mm to 0.075 mm, with no particles retained on the No. 4 sieve, indicating the absence of gravel-sized material.

Soil retention began at the No. 10 sieve (2.0 mm), accounting for 1.43% of the total mass, and increased significantly at the No. 20 and No. 40 sieves, with cumulative retention values of 8.83% and 19.60%, respectively. The maximum retention occurred at the No. 100 sieve (0.15 mm), representing 32.30% of the sample. A substantial proportion of the soil (65.93%) passed the No. 200 sieve, confirming the dominance of fine-grained particles.

The corresponding grain size distribution curve (Fig. 4) displays a smooth and continuous profile, indicating a relatively uniform gradation without abrupt changes in particle size. The steep slope observed within the fine fraction range suggests a high content of clay and silt, which is typically associated with low permeability and high-water retention capacity. These characteristics strongly influence slope stability by facilitating pore water pressure buildup during rainfall infiltration. Based on the gradation data in Table 4, the soil is composed of 34.07% sand and 65.93% clay, with no gravel content. This classification confirms that the soil is fine-grained and plastic in nature, making it highly sensitive to moisture variations and prone to strength degradation under saturated conditions.

Table 3. Soil Grain Size Distribution Data

Sieve number	Retained weight	Total retained weight [g]	Percent retained (%)	Escaped (%)	Grain diameter [mm]
4	0.0	0.000	0.00	100.00	4.75
10	4.3	4.300	1.43	98.57	2
20	22.2	26.500	8.83	91.17	0.84
40	32.3	58.800	19.60	80.40	0.42
100	38.1	96.900	32.30	67.70	0.15
200	5.3	102.200	34.07	65.93	0.075
PAN	197.8	300	100.00	0.00	

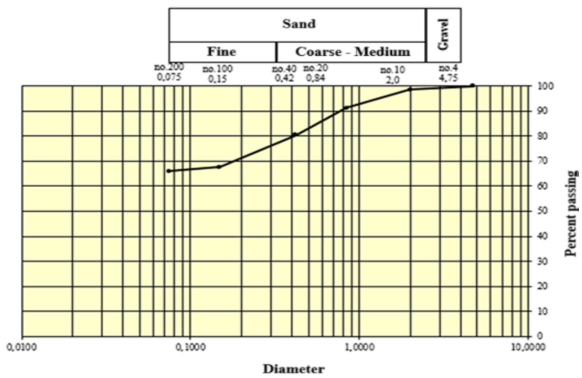

Fig.4 Soil grain distribution graph

Table 4. Summary of Soil Gradation Percentages

No	Soil type	Percentage (%)
1	Gravel	0
2	Sand	34.07
3	Clay	65.93

4.2 Effects of Increasing Water Content on Liquid Limit and Mechanical Properties

The influence of water content on soil consistency and mechanical behaviour was evaluated through laboratory testing and physical slope modelling.

Slope deformation and failure processes were continuously recorded using video documentation. Meanwhile, soil moisture content was measured at different stages of rainfall simulation.

The results indicate that increasing water content significantly affects the Liquid Limit (LL) and Plastic Limit (PL) values, leading to changes in soil plasticity and shear strength. As moisture content approached the Liquid Limit, soil stiffness decreased noticeably. resulting in progressive deformation. Once the water content exceeded the LL, the soil transitioned into a viscous, fluid-like state indicated by a significant loss of cohesion and internal friction

The experimental data presented in Table 5 show that the average reduction of water content was approximately 47.85%. which closely corresponds to the measured Liquid Limit. This observation confirms that slope failure initiation is strongly correlated with moisture content near or exceeding the LL. Furthermore, the correlation between water content and the number of blows in the Casagrande test illustrated in Fig. 5, follows a logarithmic trend, further validating the consistency limits obtained.

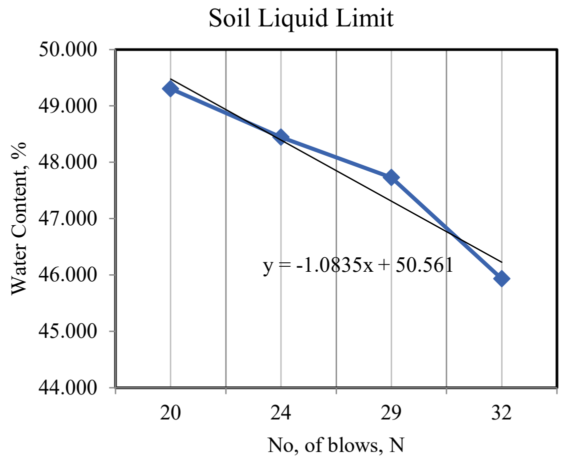

Fig.5 Liquid limit test results

Table 5. Liquid Limit and Plastic Limit Test Results

No	Type of Inspection	Liquid Limit				Plastic Limit	
	Many of strokes	20	24	29	32	A	B
1	Weight of Cup + Wet Soil	8.55	7.54	8.05	10.23	6.94	7.07
2	Weight of Cup + Dry Soil	7.13	6.45	6.79	8.31	6.21	6.52
3	Weight of Water: (1-2)	1.42	1.09	1.26	1.92	0.73	0.55
4	Weight of Cup	4.25	4.2	4.15	4.13	4.24	5.14
5	Weight of Dry Soil: (2-4)	2.88	2.25	2.64	4.18	1.97	1.38
6	Water content: (3 : 5) x 100 (%)	49.306	48.444	47.727	45.933	37.056	39.855
7	Average collapse water content (%) :	47.853				38.455	

4.3 Liquidity Index Evolution and Slope Failure Behavior

The results of the Liquidity Index (LI) tests obtained in this experiment are presented in Figs. 6–9. A detailed discussion of the observed test results is provided in the following section.

The Liquidity Index (LI) demonstrated considerable efficacy as parameter for indicating the progression of soil behavior from a stable to an unstable state. Across all slope configurations, LI values increased sharply as water content rose during rainfall simulation. Slope failure consistently occurred when LI exceeded unity indicating a transition to liquid-like state.

For the slope inclined at 30°, failure was initiated once the moisture content exceeded the soil's Liquid Limit, with LI values rapidly increasing beyond unity. Continued saturation resulted in a quasi-liquid state, ultimately leading to total slope collapse. Although gentler slopes required higher moisture content to fail, the results demonstrate that even moderate slopes can become unstable once the soil reaches a liquid consistency.

In the 45° slope model, deformation occurred at lower moisture contents compared to the 30° slope, highlighting the combined influence of slope geometry and soil consistency. Partial failure began before the Liquid Limit was reached while the total collapse occurred once LI exceeded 1, indicating a plastic-to-liquid transition.

The models with slopes of 60° and 90° demonstrated extreme sensitivity to moisture increase. In these cases, small increments in water content caused rapid increases in LI and immediate reductions in shear strength. Failure occurred abruptly once the Liquid Limit was exceeded, with LI values reaching as high as 12.9 for the 60° slope and 28.4 for the vertical slope. These results demonstrate that steep slopes are particularly vulnerable to rainfall-induced liquefaction and flow-type failures.

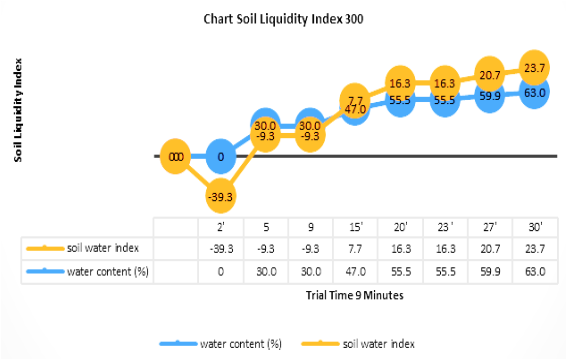

Fig.6 Soil liquidity index for slope 30º

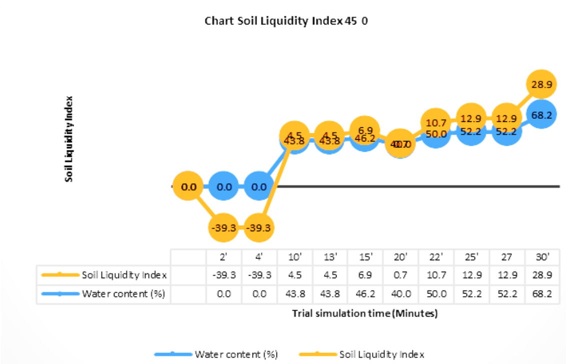

Fig.7 Soil liquidity index for slope 45º

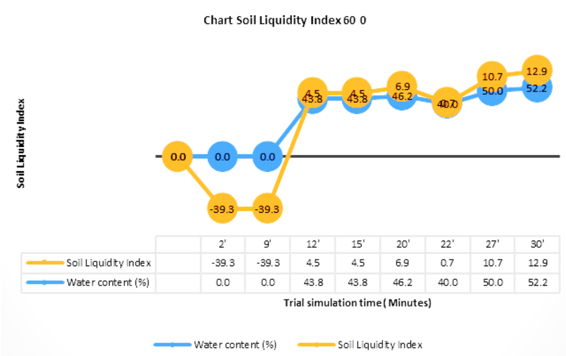

Fig.8 Soil liquidity index for slope 60º

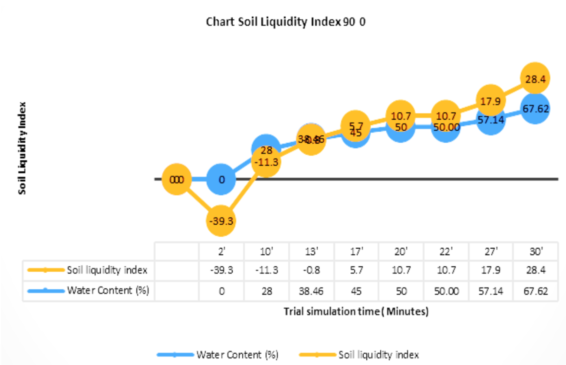

Fig.9 Soil liquidity index for slope 90º

4.4 Effect of Slope Geometry on Failure

Slope geometry significantly influences both the timing and mode of failure. Gentler slopes tend to experience progressive deformation and delayed collapse whereas steeper slopes fail rapidly once critical moisture thresholds are exceeded. As slope angle increases, gravitational forces intensify the effects of reduced shear strength making failure more sudden and severe.

The experimental results show that for steep slopes the Liquidity Index increases more rapidly with moisture content accelerating the loss of soil structure. This interaction between slope angle and soil liquidity underscores the importance of incorporating both geometric and hydraulic factors in slope stability assessments.

4.5 Mechanism of Rainfall-Induced Slope Failure

The dominant failure mechanism observed in this study is moisture-induced liquefaction resulting from excessive pore water pressure. As water infiltrates the soil matrix, matric suction decreases, particle bonding weakens, and effective stress is reduced. When the water content exceeds the Liquid Limit, soil particles lose contact, cohesion approaches zero, and the soil behaves as a viscous fluid.

Under these conditions. even minimal gravitational forces can initiate slope movement. particularly on steep slopes. Additionally, external disturbances such as prolonged rainfall or seismic vibrations can further accelerate failure leading to rapid flow-type landslides.

5. CONCLUSIONS

This study demonstrates that soil moisture content and slope geometry are the primary factors influencing slope failure mechanisms in fine-grained soils. Laboratory-scale physical modelling confirms that increasing water content significantly alters soil consistency leading to reductions in shear strength and cohesion as the Liquid Limit is approached and surpassed.

Experimental data consistently show that slope failure occurs when the Liquidity Index exceeds 1. marking the transition from plastic to liquid soil behaviour. Steep slopes (60° and 90°) exhibit particularly high vulnerability with abrupt failure occurring at relatively small increases in moisture content. The maximum recorded Liquidity Index reached 28.4 for the vertical slope indicating complete soil liquefaction and total loss of structural resistance.

The findings validate the Liquidity Index as a reliable and practical indicator for assessing rainfall-induced slope failure risk in cohesive soils. Incorporating LI into slope monitoring and early warning systems provides a simple, cost-effective. and field-applicable approach for identifying critical moisture thresholds. This research contributes to have a better understanding of slope instability mechanisms and offers valuable guidance for geotechnical risk assessment and landslide mitigation in moisture-prone terrains.

6. ACKNOWLEDGMENTS

The author expresses their deepest gratitude for the moral and financial support provided by Andalas University through the PDD Grant with the Contract No.: 28/UN16.19/PT.01.03/PDD/ 2024. on July 17. 2024.

7. REFERENCES

1. Wang G., Zhao B., Wu B., Zhang C. and Liu W., Intelligent prediction of slope stability based on visual exploratory data analysis of 77 in situ cases. International Journal of Mining Science and Technology, 33(1), 2023, pp.47–59. https://doi.org/10.1016/j.ijmst.2022.07.002.
2. Jasim O. H. and Tonaroğlu M., Using geogrid encased granular columns for embankment's slope protection: 3D-finite difference analysis. Applied Sciences, 13(4), 2023, p.2448. https://doi.org/10.3390/app13042448.
3. Vasudha G. and Deepa J., Landslide vulnerability of urban slums: Case of Warje Slum, Pune, Maharashtra. Disaster Advances, 16(3), 2023, pp.44–51. https://doi.org/10.25303/1603da044051.
4. Sestras P., Popescu C. A., Bilașco Ș., Roșca S., Cîmpeanu S. M. and Bondrea M. V., Multi-instrumental approach to slope failure monitoring in a landslide susceptible newly built-up area: Topo-geodetic survey, UAV 3D modelling and ground-penetrating radar. Remote Sensing, 14(22), 2022, p.5822. https://doi.org/10.3390/rs14225822.
5. Ma J., Li X., Zhang Y., Wang J. and Li H., Machine learning models for slope stability classification of circular mode failure: An updated database and automated machine learning (AutoML) approach. Sensors, 22(23), 2022, p.9166. https://doi.org/10.3390/s22239166.
6. Jyothi K. B. and Singh U. K., Static and pseudo-static stability analysis of right earthen embankment of Nagarjuna Sagar Dam by GeoStudio. E3S Web of Conferences, 391, 2023, p.01018. https://doi.org/10.1051/e3sconf/202339101018.
7. Wang H., Wang M., Huang Y., Mei N., and Dai X. Coupling Experimental Data With Monte Carlo Simulation And Ai For Realistic Prediction Of Slope Instability. GEOMATE Journal, 29(132), 2025, pp. 134–141. https://doi.org/10.21660/2025.132.4996.
8. Munawir A.. The Slope Stability Of Sand Slope With Two Rows Pile Reinforcing. GEOMATE Journal, 24(103), 2023, pp.52–59. https://doi.org/10.21660/2023.103.3572.
9. Zhang Z., Qin, L., Ye G., Wang W. and Zhang J., Physical modeling and intelligent prediction for instability of high backfill slope moisturized under the influence of rainfall disasters. Applied Sciences, 13(7), 2023, p.4218. https://doi.org/10.3390/app13074218.
10. Liu X. and Su M., Double strength reduction method for slope stability analysis based on water content variation: A study and engineering application. Water (Switzerland), 15(6), 2023, p.1194. https://doi.org/10.3390/w15061194.
11. Artykbaev D., Jumabayev A., Tleubayeva A. and Tleulenova G., Method for earthquake-resistant slope steepness: An integrated experimental-numerical approach. International Journal of GEOMATE, 29(131), 2025, pp.67–75. https://doi.org/10.21660/2025.131.4889.
12. Kang Q., Xia Y., Li X., Zhang W. and Feng, C., Study on the effect of moisture content and dry density on shear strength of silty clay based on direct shear test. Advances in Civil Engineering, 2022, pp.1–10. https://doi.org/10.1155/2022/2213363.
13. Ahmad W. and Uchimura T., The effect of moisture content at compaction and grain size distribution on the shear strength of unsaturated soils. Sustainability, 15(6), 2023, p.5123. https://doi.org/10.3390/su15065123.
14. Hu D., Kato S., and KIM B. S. Evaluation Of Infinite Slope Stability With Various Soils Under Wet-Dry Cycle. GEOMATE Journal, 26(115), 2024, pp. 89–99. https://doi.org/10.21660/2024.115.g13306.
15. Murison R. A., Jacobsz S. W., Gaspar T. A. V., Burke T. S. D. S and Osman A. S., Drying and wetting soil-water retention behaviour of a highly expansive clay under varying initial density. E3S Web of Conferences, 382, 2023, p.09005. https://doi.org/10.1051/e3sconf/202338209005.
16. Xu Y., Zhang X., Wang G., Liu X. and Yang A., Role of diatom microstructure in determining the Atterberg limits of fine-grained diatomaceous soil. Applied Sciences, 13(4), 2023, p.2287. https://doi.org/10.3390/app13042287.
17. O'Kelly B. C., Alonso-Azcárate J. and Moreno-Maroto J. M., A comprehensive review of soil remolding toughness determination and its use in the classification of fine-grained soils. Applied Sciences, 13(9), 2023, p.5711. https://doi.org/10.3390/app13095711.
18. Jiang J. J. and Cui Z. D., Instability of high liquid limit soil slope for the expressway induced by

rainfall. Applied Sciences, 12(21), 2022, p.10857. https://doi.org/10.3390/app122110857.
19. Feng X., Effect of shear rate on the residual strength of clayey soils. Journal of Electrical Systems, 20(3), 2024, pp.1835–1841. https://doi.org/10.52783/jes.3749.
20. Troncone A., Pugliese L. and Conte E., Rainfall threshold for shallow landslide triggering due to rising water table. Water (Switzerland), 14(19), 2022, p.2966. https://doi.org/10.3390/w14192966.
21. Hakro M. R., Almani Z., Channa M. A. and Jokhio J., Numerical modelling of matric suction in unsaturated soil under shallow foundation under varying soil and hydrological conditions. Jurnal Kejuruteraan, 36(2), 2024, pp.569–580. https://doi.org/10.17576/jkukm-2024-36(2)-17.
22. Ling J., Li X., Lin S., Cen Y. and Li C., Laboratory study on entire range suction measurement and microstructure change of granite residual soil. Transportation Research Record, 2677(10), 2023, pp.191–203. https://doi.org/10.1177/03611981231160546.
23. Adiguna G. A., Wijaya M., Rahardjo, P. P., Sugianto A., Satyanaga A. and Hamdany A. H., Practical approach for assessing wetting-induced slope failure. Applied Sciences, 13(3), 2023, p.1811. https://doi.org/10.3390/app13031811.
24. Rahardjo H., Ong, T. H., Rezaur R. B. and Leong E. C., Factors controlling instability of homogeneous soil slopes under rainfall. Journal of Geotechnical and Geoenvironmental Engineering, 133(12), 2007, pp.1532–1543. https://doi.org/10.1061/(ASCE)1090-0241(2007)133:12(1532).
25. Sugimoto S. and Ishizuka Y., Slope deformation monitoring using wireless sensor network and evaluation of mechanical stability by FDM simulation. International Journal of GEOMATE, 22(94), 2022, pp.13–20. https://doi.org/10.21660/2022.94.97.
26. Nofrizal, Fauzan, Hakam A., Istijono B. I. and Aprisal, Analysis of the effect of rainfall intensity and slope steepness on landslide disaster. Civil and Environmental Engineering, 21(2), 2025, pp.959-973. https://doi.org/10.2478/cee-2025-0073.
27. Dewanto B. G., Supendi P., Nugraha A. D., Widiyantoro S., Rosalia S. and Sahara D. P., The 2022 Mw 6.1 West Pasaman, Indonesia earthquake confirmed the existence of the Talamau Segment Fault based on teleseismic and satellite gravity data. Quaternary, 5(4), 2022, p.45. https://doi.org/10.3390/quat5040045.
28. Hoa P. V., Tuan N. Q., Hong P. V., Thao G. T. P. and Binh N. A., GIS-based modeling of landslide susceptibility zonation by integrating the frequency ratio and objective–subjective weighting approach: A case study in a tropical monsoon climate region. Frontiers in Environmental Science, 11, 2023, pp.1–20. https://doi.org/10.3389/fenvs.2023.1175567.
29. Das B. M., Principles of Geotechnical Engineering, 7th ed., Cengage Learning, Stamford, CT, USA, 2010, pp.1–500.